Figure Legends

Supplementary Figure 1: Effect of myoV-HMM on the spectrum of deac-aminoADP

Excitation/emission spectra profiles of 0.5 μM deac-aminoADP in solution in the presence and the absence of 1 μM myoV-HMM. In the presence of myoV-HMM, the intensities of the emission (blue) and excitation (black) spectrum are 25X higher than in the absence of myoV-HMM (red and green, respectively). The inset shows a magnified intensity profile of deac-aminoADP (0.5 μM) in the absence of myoV-HMM. Experimental conditions were 40 mM KCl, 20 mM MOPS, 4 mM $MgCl_2$, 0.1 mM EGTA, 1 μM calmodulin, 50 mM DTT pH 7.5, 25^o C, containing the same oxygen scavenging system described in Fig. 3.

Supplementary Figure 2: Run lengths and velocity of AlexaFluor568-myoV-HMM.

a, Histograms of the run lengths of AlexaFluor568-myoV-HMM were measured with 1 mM ATP (black closed circles) or 1 mM deac-aminoATP (red closed circles). The solid lines represent the exponential fits of the run length distribution. The mean and S.D. of run length with ATP and deac-aminoATP are 1950 ± 160 nm (r^2 = 0.93) and 1050 ± 80 nm (r^2 = 0.96); b, velocity of myoV-HMM movement on actin at various deac-aminoATP concentrations. The maximum velocity is 120 nm/s. *Inset* shows the data over the range of 50 nM to 1000 nM deac-aminoATP. Conditions are as described in Fig. 2 legend.

Supplementary Figure 3: Dependence of the measured intensity of photons upon camera gain. Values of deac-aminoADP intensities in the presence (closed circles) and absence (open circles) of myoV-HMM on the surface of the slide. Intensity values of AlexaFluor568-myoV-

HMM are shown by open squares. The red line represents the number of photons required for FIONA measurements with a resolution of 2.5 nm. Note that under these conditions in the microscope we see around a 4-fold increase in intensity when deac-aminoADP binds to myoV-HMM which is smaller than the 25-fold increase found using the spectrofluorimeter in solution. Reasons for this probably include choice of filter sets, lower protein concentration and scattering artifacts.

Supplementary Figure 4: Photobleaching experiments of deac-aminoADP, AlexaFluor568-labeled-calmodulin, and AlexaFluor568-labeled-myoV-HMM.

a) and b) Deac-aminoADP bound to myoV-HMM, which is bound to nitrocellulose-coated coverslip surface, show one and two photobleaching events, respectively. c) Photobleaching of AlexaFluor568-labeled-calmodulin nonspecifically bound to the surface. In this example two photobleaching events were detected. d) and e), Photobleaching of AlexaFluor568-labeled-myoV-HMM. Individual photobleaching events are not so clear, but initial intensities are proportional to the number of fluorophors. f) histogram of numbers of Alexafluor568 dyes per molecule. The initial intensities of AlexaFluor568-calmodulin and AlexaFluor568-myoV-HMM were normalized to the averaged intensity of a single AlexaFluor568 dye. The means of fluorescent labeling ratio of calmodulin and myoV-HMM are 1.9 and 6.1 dyes per molecule, respectively which is in good agreement from values measured in solution using the appropriate extinction coefficients (see above).

Supplementary Figure 5: Additional samples of stepping traces and nucleotide intensities of AlexaFluor568-myoV-HMM and deac-aminoATP. a) and b) 100 nM deac-aminoATP, c)

200 nM deac-aminoATP. This trace is the data from the Movie (below). d) 400 nM deac-aminoATP. In each set the top trace is the movement of AlexFluor568-myoV-HMM. The middle trace is the movement of the deac-aminonucleotide. The bottom trace is the normalized fluorescence intensity of the spots as a function of time. The red vertical dashed lines represent coincidental stepping events of AlexaFluro568- myoV-HMM and deac-aminonucleotide fluorescence. The blue vertical lines represent stepping events of just the deac-aminonucleotide fluorescence. Conditions are as described in Fig. 2 legend.

Supplementary Figure 6: **AlexaFluor568-myoV-HMM and deac-amino-nucleotide move together along the actin filament.**

Panel a is a summed stack (300 frames) from a movie which shows a field of AlexaFluor568-myoV-HMM molecules moving on actin filaments in the presence of deac-aminoATP. Panel b is a summed stack (300 frames) made from imaging the deac-aminonucleotide fluorescence for the same movie. Both images are shown in reverse contrast for clarity. Similar tracks are seen for the two fluorophors.

Supplementary Figure 7: Sample of an asymmetric stepping trace of Alexafluor568-myoV-HMM moving along actin. The two motor domains of individual HMM molecules could contain different numbers of AlexaFluor568 dyes and this would result in asymmetric stepping traces where the sum of two sequential movements equal 72 nm. An example of such a trace taken at highest camera gain (1000) and 400 nM deac-aminoATP is shown. Conditions are as described in Fig.2 legend.

Supplementary Figure 8: Histogram of integrated intensities of deac-amino nucleotide fluorescence during processive movement of myoV-HMM.

Data (n = 273) were obtained from a series of experiments identical to those described in Fig. 2 and 3 of the main manuscript. The lower intensity peak corresponds to one deac-aminonucleotide molecule bound to myoV-HMM and the larger intensity peak to two bound deac-aminonucleotides bound to one myoV-HMM. Conditions are as described in Fig. 2 legend.

Supplementary Figure 9. Kinetics of deac-aminoATP binding and deac-aminoADP dissociation from the actomyoV-S1 We did solution kinetic studies of deac-aminoATP binding and deac-aminoADP dissociation with single headed actomyoV-S1. The kinetics are simpler on the one headed molecule and we had previously shown that nucleotide binding and dissociation kinetics are the same for actomyoV-S1 and the trailing head of actomyoV-HMM[10]. A. MyoV-S1 was mixed with deac-aminoATP, held 20 s in a delay line, and then mixed with phalloidin-actin and an ATP chase and the data collected vs log time ($\lambda_{excitation}$ = 430 nm and $\lambda_{emission}$ >450 nm). Experimental conditions were identical to those used in single molecule experiments (Fig. 2): 20 mM MOPS, 4 mM $MgCl_2$, 40 mM KCl, 0.1 mM EGTA, 50 mM DTT, pH 7.5, 25°C. The solid line through the average of 4 data sets is the best fit to a single exponential equation: $I(t) = I_o e^{-1.26t} + C$. Final concentrations of protein and nucleotides in the cell: 0.25 μM myoV-S1, 0.25 μM deac-aminonucleotide, 11.2 μM actin and 1.2 mM ATP. A similar rate of 1.2 s^{-1} was observed if the deac-aminoATP was incubated with the actomyoV-S1 for 120 s to allow the myoV-deacaminoADP-Pi to be converted to myoV-deac-aminoADP before mixing with actin and ADP(data not shown) B. Deac-aminoATP was mixed with actomyoV-S1 and the data collected as in A. Final concentrations in the cell: 11 nM myoV-S1, 417 nM deac-aminoATP and 0.5 μM actin The solid line through the average of 5 data sets is

the best fit to a single exponential equation: $I(t) = I_o e^{-1.31t} + C$. C. Experiments were similar to those in B except that the deac-aminoATP concentration was varied as indicated. Error on the measurement is within the size of the symbols. The line fit through the data has a slope of 2.48 +/-0 .05 $\mu M^{-1} s^{-1}$ with an intercept of 0.28 +/- 0.02 s^{-1}. The observed rate of deac-aminoADP dissociation from actomyoV of 1.26 s^{-1} (B) is indicated by the arrow.

Movie: Coincident movement of AlexaFluor568-myoV-HMM and deac-aminonucleotide. Conditions are as described in Fig. 2 legend. Left panel, AlexaFluor568-myoV-HMM; right panel, deac-aminonucleotide.

Supplementary Figure 1

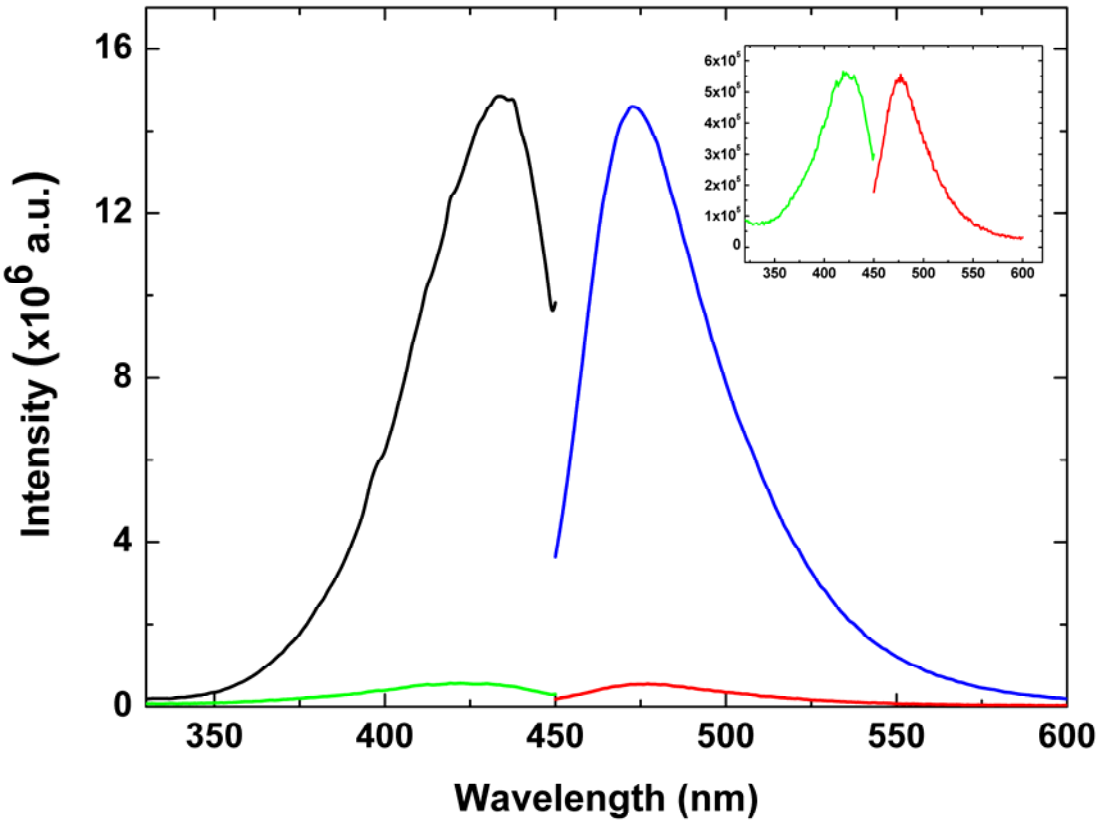

Supplementary Figure 2

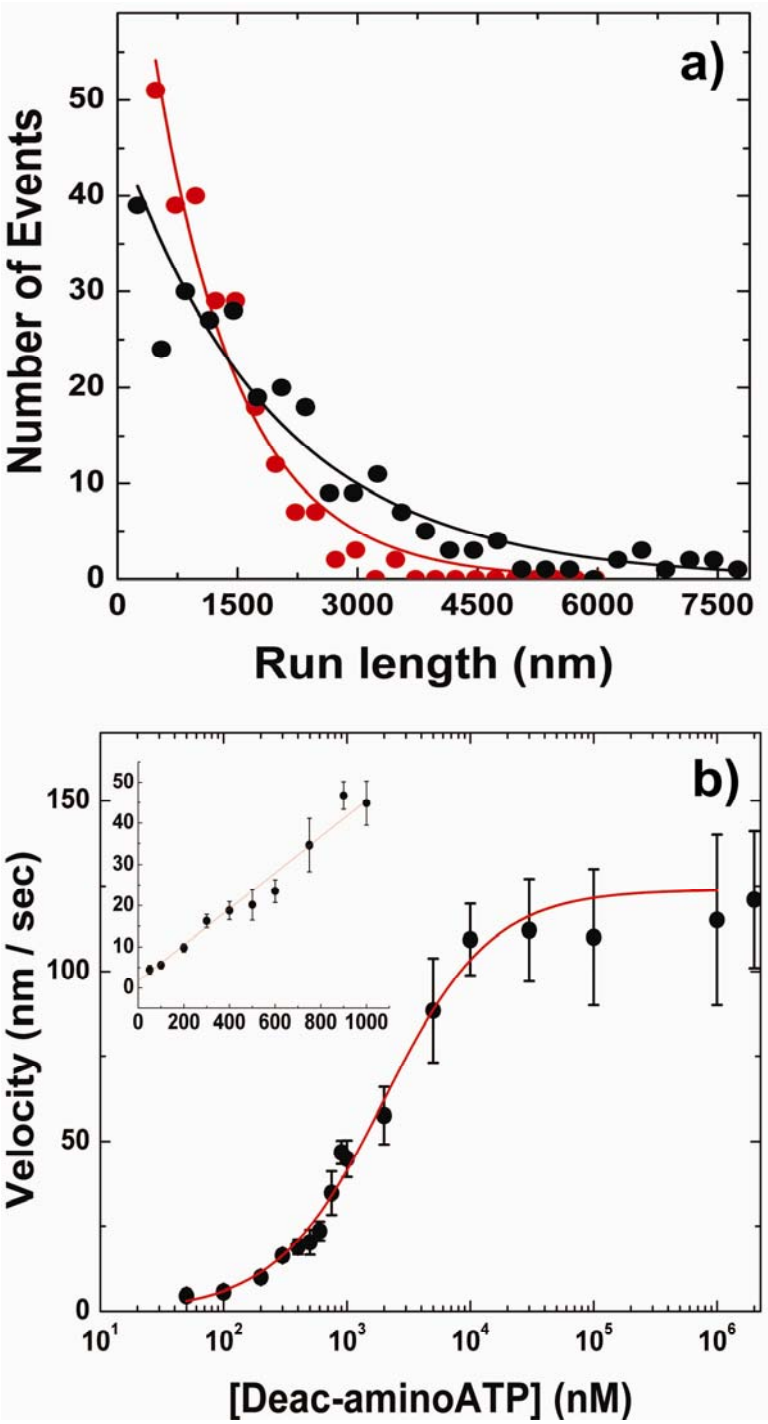

Supplementary Figure 3

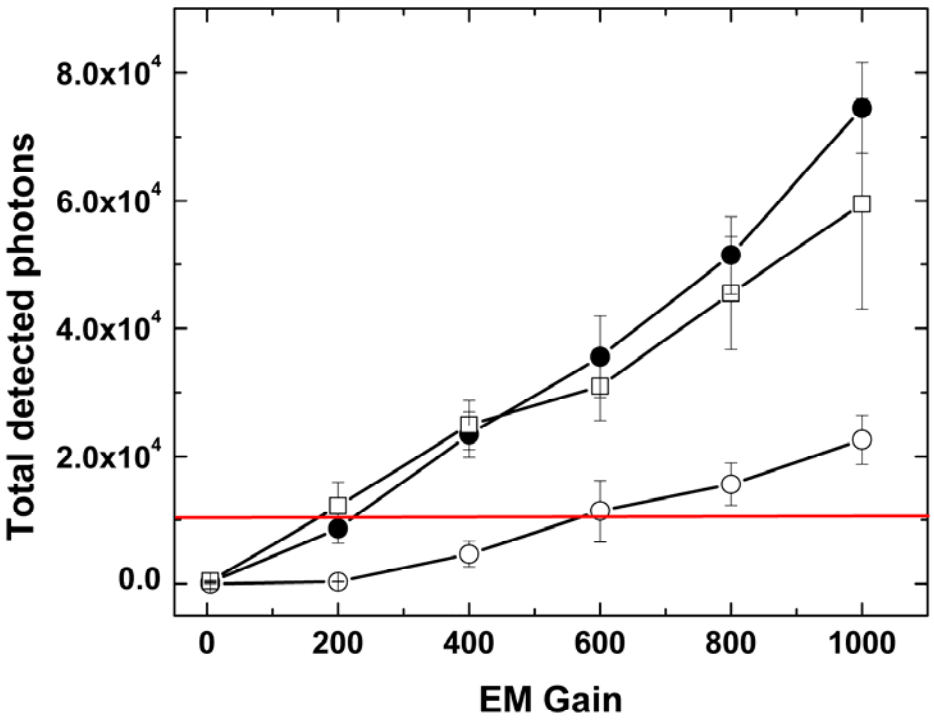

Supplementary Figure 4

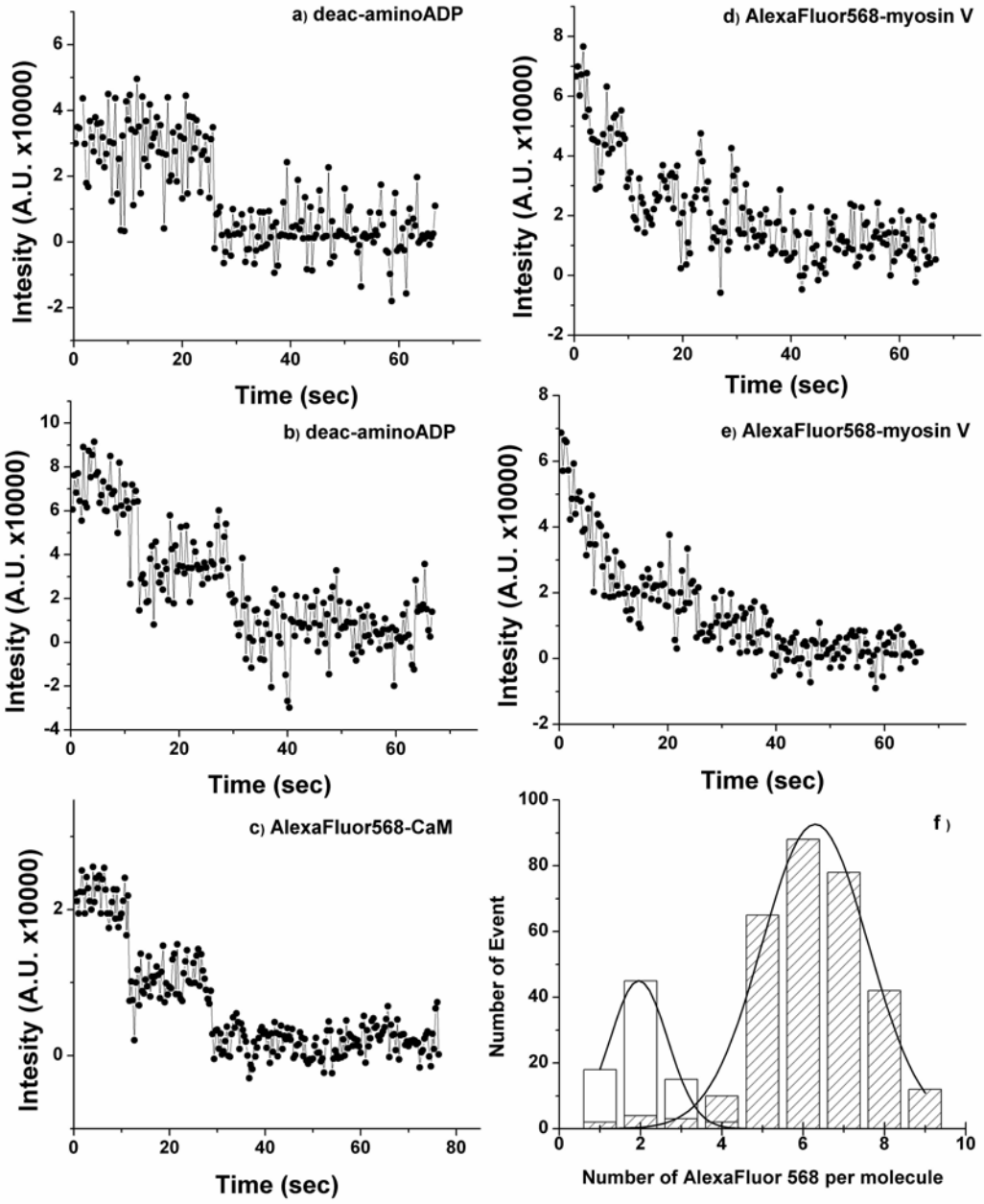

Supplementary Figure 5

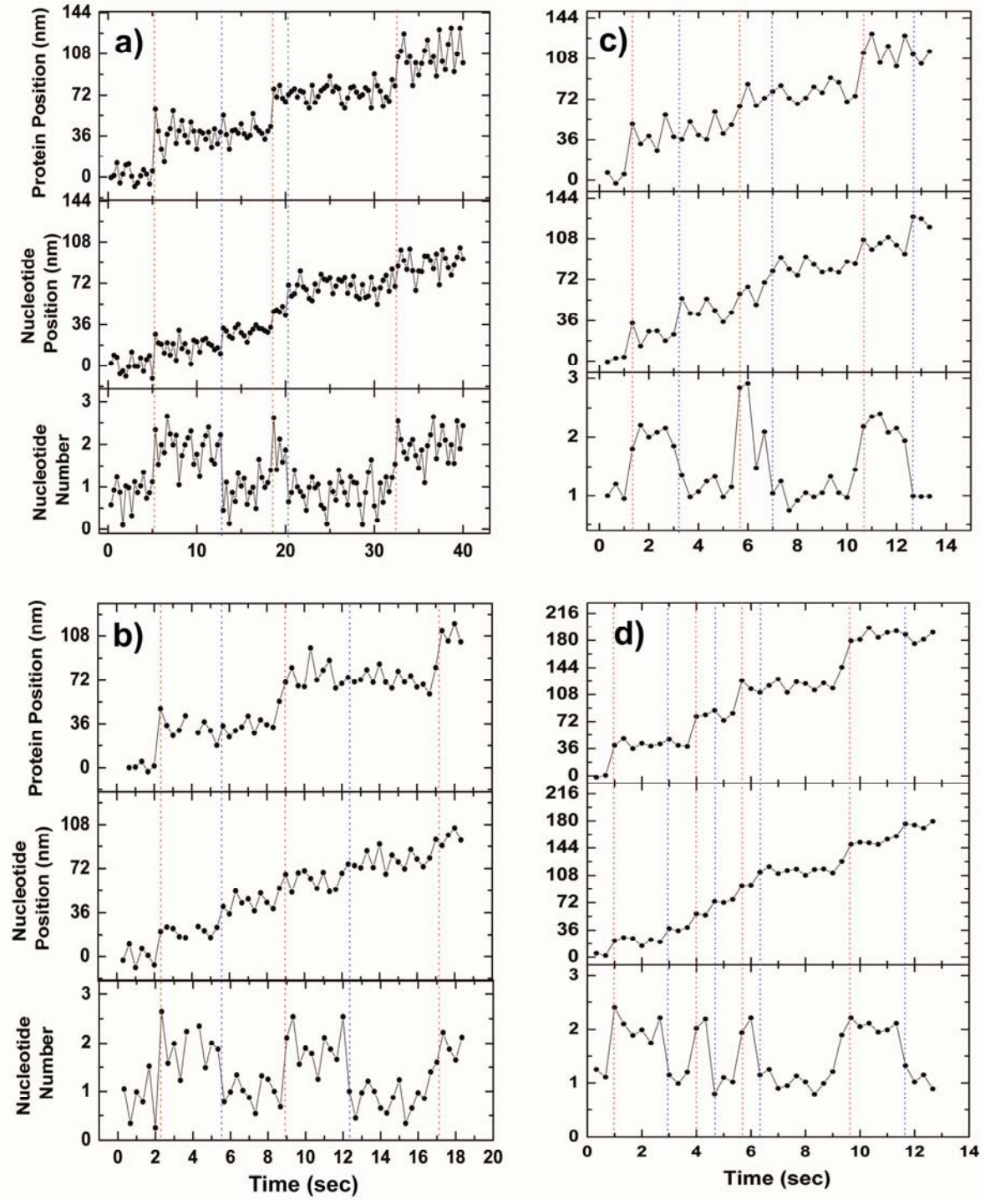

Supplementary Figure 6

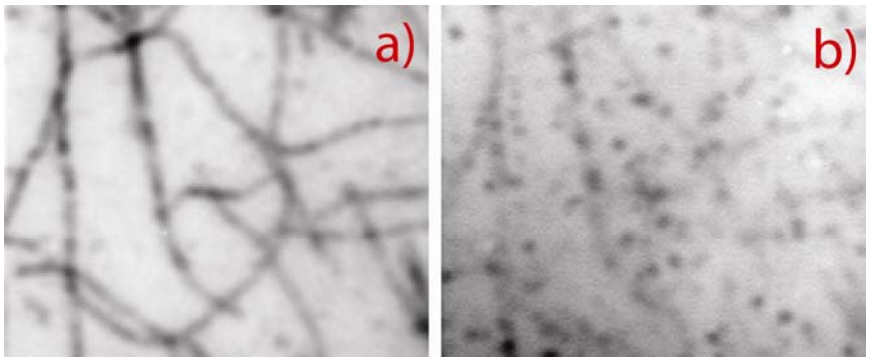

Supplementary Figure 7

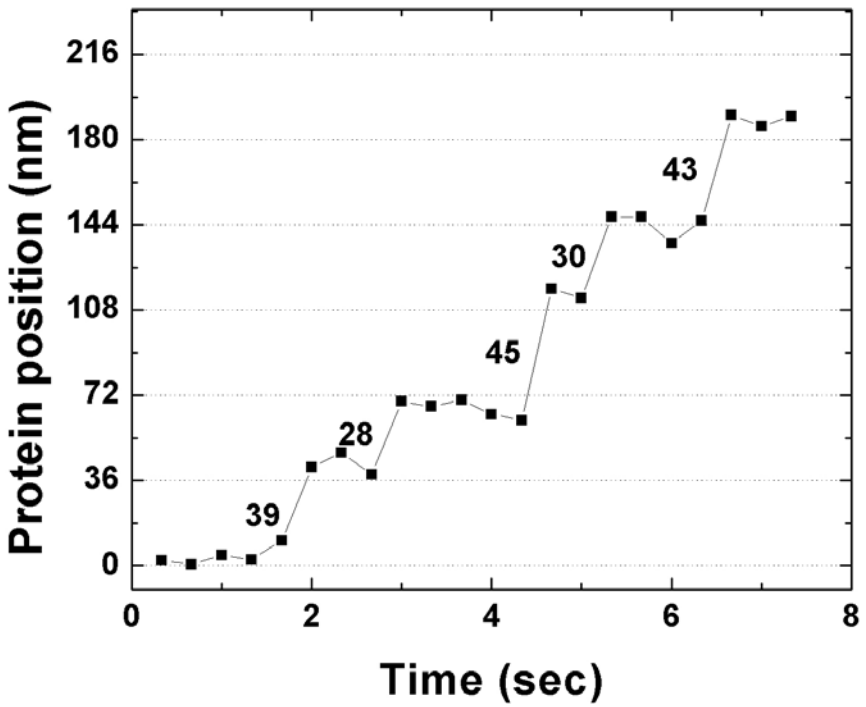

Supplementary Figure 8

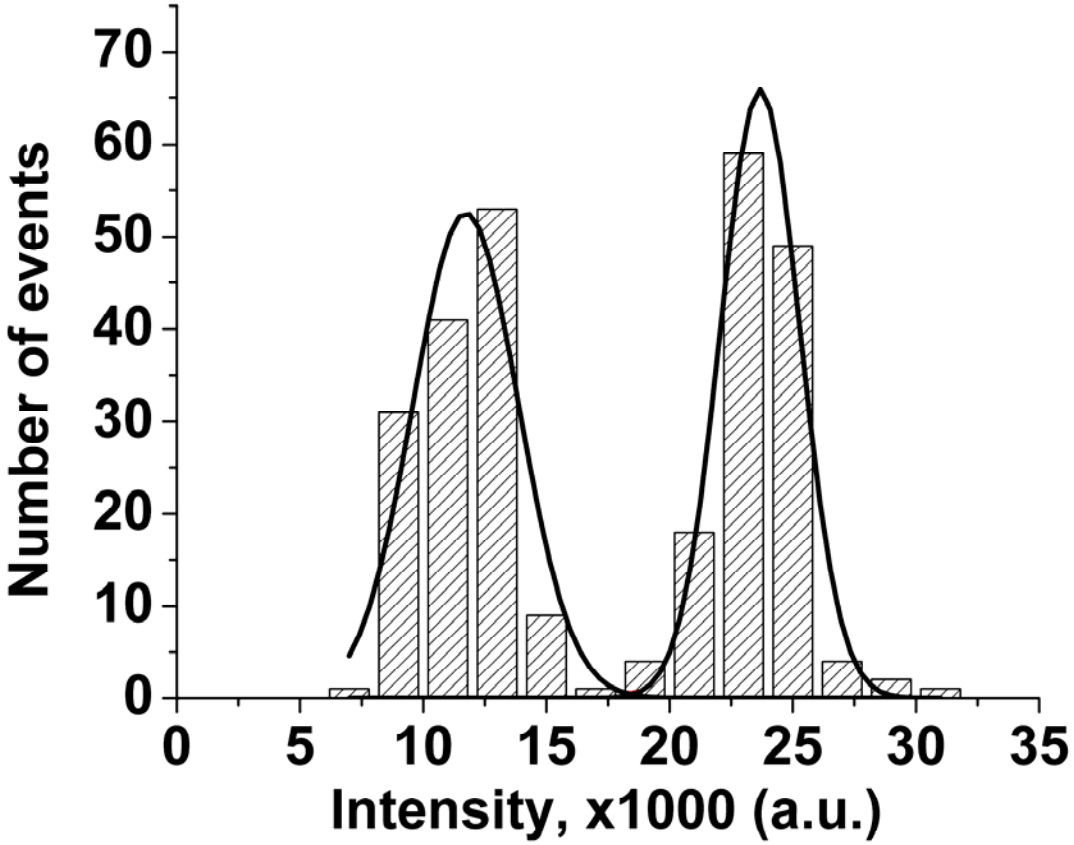

Supplementary Figure 9

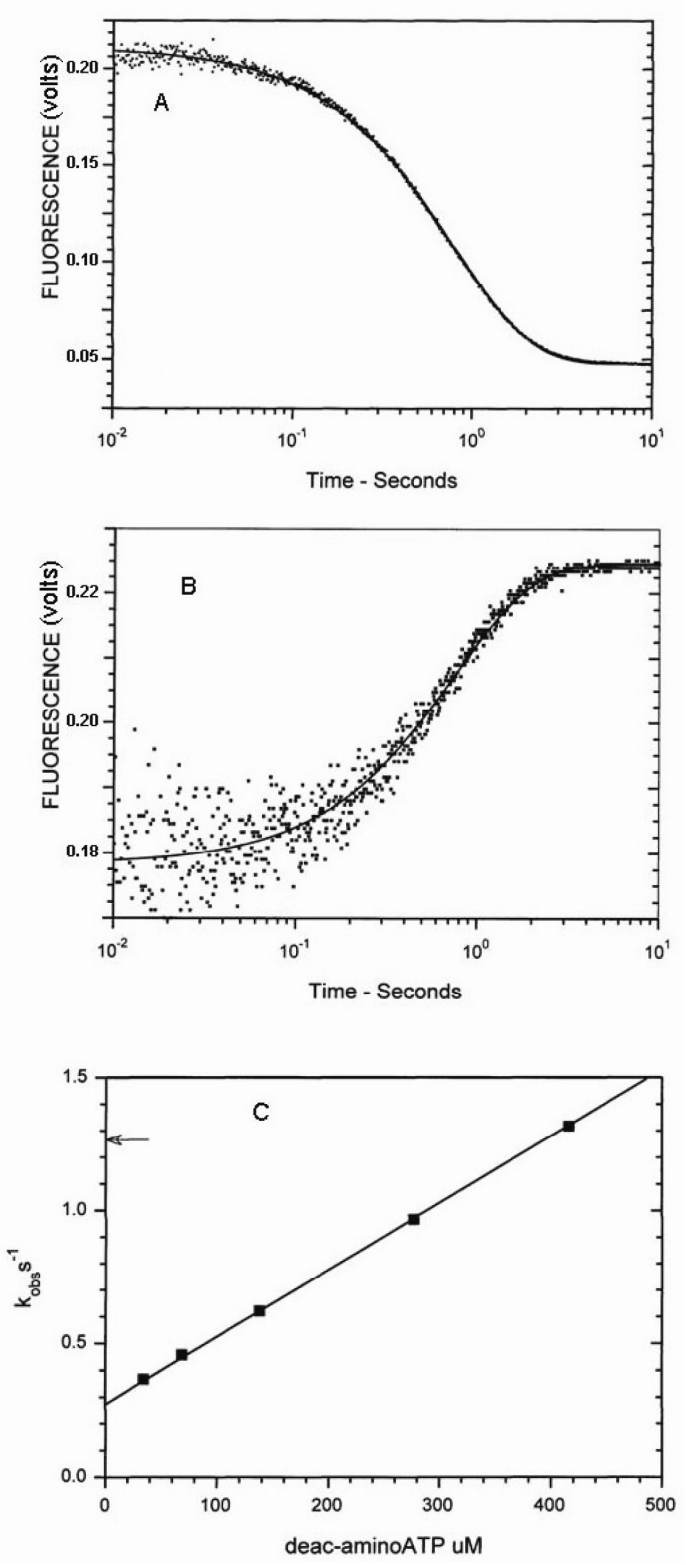

Supplementary movies